bioRxiv preprint doi: https://doi.org/10.1101/544064; this version posted February 13, 2019. The copyright holder for this preprint (which was not certified by peer review) is the author/funder, who has granted bioRxiv a license to display the preprint in perpetuity. It is made available under aCC-BY-NC-ND 4.0 International license.

Sweet revenge - *Streptococcus pyogenes* showcases first example of immune evasion through specific IgG glycan hydrolysis

Andreas Naegeli[1], Eleni Bratanis[1], Christofer Karlsson[1], Oonagh Shannon[1], Raja Kalluru[1,2], Adam Linder[1], Johan Malmström[1], Mattias Collin[1,*]

1) Lund University, Faculty of Medicine, Department of Clinical Sciences, Division of Infection Medicine, Lund, Sweden

2) Current affiliation: Department of Pathology, Stanford University School of Medicine, Stanford, California, USA.

* to whom correspondence should be addressed: Division of Infection Medicine, Department of Clinical Sciences, Biomedical Center B14, Lund University, SE-221 84 Lund, mattias.collin@med.lu.se

Abstract

Streptococcus pyogenes (Group A streptococcus, GAS) is an important human pathogen responsible for a wide variety of diseases from uncomplicated tonsillitis to life-threatening invasive infections. GAS secretes EndoS, an endoglycosidase able to specifically cleave the conserved *N*-glycan on human IgG antibodies. *In vitro*, removal of this glycan impairs IgG effector functions but its relevance to GAS infection *in vivo* is unclear. Using targeted mass spectrometry, we were able to characterize the effects of EndoS on host IgG glycosylation during the course of natural infections in human patients. We found substantial IgG glycan hydrolysis locally at site of infection as well as systemically in the most severe cases. Using these findings we were able to set up appropriate model systems to demonstrate decreased resistance to phagocytic killing of GAS lacking EndoS *in vitro,* as well as decreased virulence in a mouse model of invasive infection. This study represents the first described example of specific bacterial IgG glycan hydrolysis during infection and highlights the importance of IgG glycan hydrolysis for streptococcal pathogenesis. We thereby offer new insights into the mechanism of immune evasion employed by this pathogen with clear implications for treatment of severe GAS infections and future efforts at vaccine development.

bioRxiv preprint doi: https://doi.org/10.1101/544064; this version posted February 13, 2019. The copyright holder for this preprint (which was not certified by peer review) is the author/funder, who has granted bioRxiv a license to display the preprint in perpetuity. It is made available under aCC-BY-NC-ND 4.0 International license.

Introduction

Streptococcus pyogenes (group A streptococcus, GAS) is a human pathogen causing a diverse range of diseases. GAS can cause mild infections such as tonsillitis and impetigo but also severe diseases such as streptococcal toxic shock syndrome, necrotizing fasciitis, and erysipelas[1]. Furthermore, repeated and/or untreated GAS infections can trigger serious postinfectious immune-mediated disorders, including acute poststreptococcal glomerulonephritis, acute rheumatic fever, and rheumatic heart disease[1]. With a prevalence of at least 18 million severe cases, leading to approximately half a million deaths world wide annually as well as over 700 million annual cases of mild infections[2], GAS infections are a large public health burden.

Protective immunity towards GAS is generally poor and recurrent infections are not uncommon, especially in children[3]. This is despite the fact that most people do in fact raise an adaptive immune response and exhibit high titers of IgG antibodies towards different GAS antigens[4-7]. The reason for the lack of protection is not entirely understood but can in part be attributed to the large number of different GAS serotypes and the surface antigen variability this entails[8]. GAS is also able to counteract adaptive immunity by specifically impairing IgG function. This can be mediated by non-immune IgG binding to Fc binding proteins on the streptococcal surface such as the M and M-related proteins[9,10] or through specific degradation of the IgGs themselves. GAS secretes for example the IgG specific protease IdeS which is able to cleave the antibody in the hinge region, separating the antigen-binding Fabs from the effector function-promoting Fc region[11].

GAS is further able to degrade IgGs by secretion of the endoglycosidase EndoS. This enzyme cleaves the conserved Fc *N*-glycan from IgGs with great specificity[12] (Fig. 1a). This glycan is situated at the interaction surface between the IgG and Fc receptors[13,14] as well as the complement system[15] and is therefore ideally located to influence IgG effector function. While an antibody´s specificity is determined by the Fab regions, the Fc region determines which effector functions are elicited and the structure of the Fc glycan has been shown to be crucial in the regulation of this process[16]. For example, IgGs lacking core fucosylation exhibit increased affinity for FcγRIIIA and are therefore significantly more potent in eliciting antibody-dependent cellular cytotoxicity[17,18]. Furthermore, the degree of galactosylation of the Fc glycan influences an IgGs ability to activate the complement system[19]. Consequently, IgG antibodies lacking the Fc glycan fail to bind to most Fc receptors and are unable to

bioRxiv preprint doi: https://doi.org/10.1101/544064; this version posted February 13, 2019. The copyright holder for this preprint (which was not certified by peer review) is the author/funder, who has granted bioRxiv a license to display the preprint in perpetuity. It is made available under aCC-BY-NC-ND 4.0 International license.

activate the complement system[20,21]. Despite the accumulating evidence that antibody glycans are instrumental in regulating and fine tuning the immune response, very little is know about the role of antibody glycosylation during infections and if it contributes to the outcome of disease. However, recent high profile studies that have suggested that the IgG glycosylation status influences whether HIV infection is controlled[22,24] and whether *Mycobacterium tuberculosis* infection is active or latent[23].

Due to this functional importance of the Fc *N*-glycan, its hydrolysis by EndoS leads to impaired IgG effector functions such as Fc receptor binding and complement activation *in vitro*[20,24,25]. This would intuitively suggest a role for EndoS in evasion of adaptive immunity through perturbation of protective IgG responses. However, studies on the influence of EndoS on GAS pathogenesis have so far been few and inconclusive. They were unable to demonstrate under which conditions EndoS is expressed and active and had to rely on overexpression or addition of recombinant enzyme to manifest a virulence phenotype[25,26]. These efforts at elucidating the contribution of EndoS to GAS virulence have been hampered by the difficulty of finding relevant model systems and the lack of a sensitive analytical approach to quantify EndoS activity in complex systems[25,26] .

We therefore wanted to take a different approach by first characterizing the effect of EndoS on the hosts IgG glycosylation *in vivo* during the course of natural GAS infections in human patients and then use these results to set up relevant model system able to show how EndoS affects the hosts IgG response and how this contributes to GAS virulence. This necessitates an assay that is robust, specific, and sensitive enough to be able to quantify the glycosylation state of IgG in complex patient samples. We chose to employ selected reaction monitoring (SRM), a targeted mass spectrometry approach that is uniquely suitable for this type of analysis as it allows for the quantification of predefined target molecules (such as the EndoS reaction products) directly from highly complex samples. SRM is based on precursor peptide ion selection, fragmentation through collision, and detection of selected peptide fragment ions in a triple quadrupole mass spectrometer. Precursor/fragment pairs, so called transitions, are chosen that are unique to the molecule to be detected (i.e. the EndoS reaction products) and data is only acquired for these defined targets (for a review see Picotti et al.[27]). In previous studies, proteins with concentrations as low as 300 ng/ml have been reliably quantified out of crude human plasma preparations[28,29] and SRM has also been used successfully for quantification of the different glycan structures on IgG directly from serum samples[30].

bioRxiv preprint doi: https://doi.org/10.1101/544064; this version posted February 13, 2019. The copyright holder for this preprint (which was not certified by peer review) is the author/funder, who has granted bioRxiv a license to display the preprint in perpetuity. It is made available under aCC-BY-NC-ND 4.0 International license.

We employed SRM-MS to quantitatively assess the EndoS-mediated IgG glycan hydrolysis in samples from natural GAS infections in humans. We used these findings to set up relevant *in vitro* assays and animal models in order to demonstrate the importance of EndoS-mediated antibody modification in evasion of adaptive immunity and therefore GAS virulence.

Results

A TARGETED MASS SPECTROMETRY APPROACH FOR QUANTITATIVE ANALYSIS OF IGG GLYCAN HYDROLYSIS

In order to assess the effect of EndoS on IgG glycosylation during streptococcal infections *in vivo*, we first needed an assay powerful enough to allow us to quantify the EndoS reaction products directly from very complex samples such as patient material (plasma, wound swabs or throat swabs). Previous attempts at measuring EndoS activity relied on SDS-PAGE[31,32] or analysis of released glycans by HPLC[33]. These methods lack sensitivity, specificity and/or are ill suited for analysis of complex material. We therefore developed an SRM mass spectrometry method to specifically quantify the amount of glycan-hydrolyzed IgGs (IgG_{GH}). As EndoS cleaves within the chitobiose core of the IgG *N*-glycan (Fig. 1a), it leaves the reducing end *N*-Acetylglucosamine (GlcNAc) residue attached to the protein[34] and leads to the generation of a new IgG proteoform with a truncated glycan that is not detected in healthy individuals[35,36]. Samples were digested with trypsin and the peptides were treated with α-fucosidase to remove potential core fucosylations and end up with a single EndoS reaction product per IgG subclass. We defined SRM transitions for the tryptic peptides containing the glycosylation site of human IgG (IgG1: EEQYN(GlcNAc)STYR, IgG2: EEQFN(GlcNAc)STFR, IgG3: EEQYN(GlcNAc)STFR IgG4: EEQFN(GlcNAc)STYR) modified with a single *N*-linked GlcNAc residue. As the glycopeptides of IgG3 and IgG4 have the same precursor mass, we defined transitions that are in common and quantified both peptides together. To assess total IgG levels, previously developed SRM assays for quantification of each IgG subclass[37] were included. All the transitions are listed in Table S2. To determine the absolute amounts of IgG and IgG_{GH}, we synthesized heavy-isotope labeled standard peptides corresponding to the peptides we analyzed, which could be spiked into the samples to act as internal standards (Fig. 1b). The method was calibrated using a defined human standard serum (Fig. S1&2, Table S3) and validated by analyzing a set of human blood plasma samples with defined amounts of IgG_{GH}. For method comparison, the same samples were also analyzed by SDS-PAGE and *Lens culinaris* agglutinin (LCA) lectin blot

bioRxiv preprint doi: https://doi.org/10.1101/544064; this version posted February 13, 2019. The copyright holder for this preprint (which was not certified by peer review) is the author/funder, who has granted bioRxiv a license to display the preprint in perpetuity. It is made available under aCC-BY-NC-ND 4.0 International license.

(Fig. 1cd). The SRM method exhibited better precision and accuracy as well as a much lower detection limit. Especially for samples where the IgG_{GH} content was low, as might be expected in clinical samples, the SRM method outperformed the SDS-PAGE assay. This together with low sample requirements, a large dynamic range and high analytical precision (Fig. S1, S2) made this method highly suitable for the analysis of complex patient materials. With this, method development was complete and we could start measuring EndoS activity during GAS infections *in vivo*.

IgG glycans are hydrolyzed during GAS tonsillitis

Tonsillitis is the most common form of GAS infection and is characterized by throat pain, fever, tonsillar exudates and cervical lymph node adenopathy[1]. To study the effects of EndoS on patient IgGs during such an infection, we obtained 59 throat swab samples from a total of 54 patients who sought medical attention for a sore throat (Fig. 2a). 26 of these were diagnosed with GAS tonsillitis by rapid strep test and/or throat culture and were prescribed oral antibiotics. The other 28 patients exhibited a negative strep test and throat culture; therefore the infection was suspected to be viral and left untreated. 5 of the patients diagnosed with GAS tonsillitis were willing to return after antibiotic treatment and an additional throat swab was collected for each of these (Fig. 2a)

We used SRM mass spectrometry to quantitatively analyze the levels of IgGs as well as their glycosylation status in these throat swab samples. We observed no difference between GAS-positive and GAS-negative patients in total IgG content or in the distribution of the four IgG subclasses (data not shown). However, the percentage of glycan-hydrolyzed IgGs was significantly higher in the GAS tonsillitis group, with glycan hydrolysis approaching 80% in one case (Fig. 2b, left panel). This was no longer detectable in any of the samples taken after antibiotic treatment (Fig. 2b, right panel). Furthermore, IgG glycan hydrolysis could be correlated to the grade of throat pain and the general malaise experienced by the patients as well as their Centor scores (a clinical scoring system aimed at distinguishing GAS tonsillitis from viral infections[38]) (Fig. 2c). Taken together, these results suggest that EndoS is expressed and active during acute GAS tonsillitis, but its effects quickly disappear upon therapeutic intervention.

IgG antibodies are deglycosylated systemically during GAS induced sepsis

Sepsis is a state of systemic inflammation in response to an infection and the worst case scenario in GAS infections[1]. To address the effect of EndoS on patient IgG antibodies during

bioRxiv preprint doi: https://doi.org/10.1101/544064; this version posted February 13, 2019. The copyright holder for this preprint (which was not certified by peer review) is the author/funder, who has granted bioRxiv a license to display the preprint in perpetuity. It is made available under aCC-BY-NC-ND 4.0 International license.

159 invasive GAS infection leading to sepsis, we collected blood plasma from 32 patients
160 suffering from sepsis of various degrees of severity as well as 12 healthy volunteers. 18
161 patients had confirmed GAS infections whereas the other 14 suffered from various other
162 bacterial infections (Fig. 3a, table S5). All the sepsis patients were ranked according to the
163 degree of severity of their condition (sepsis, severe sepsis or septic shock). We used our SRM
164 method to determine IgG levels and glycosylation state in blood plasma (Fig. 3b, table S5).
165 The total IgG levels were not significantly different between the groups (Fig. 3b) and no
166 appreciable amounts of glycan-hydrolyzed IgG could be detected in any of the plasma
167 samples from the control groups (healthy or non-GAS sepsis). The same was true for milder
168 cases of GAS induced sepsis. However, the plasma of 5 out of 6 GAS patients suffering from
169 septic shock contained significantly increased amounts of IgG_{GH} (up to 1 mg/ml in the most
170 severe case) (Fig. 3b).

171 As we observed large differences in IgG glycan hydrolysis, even among the septic shock
172 patients, we hypothesized that differential expression of EndoS among the different GAS
173 strains infecting these patients could account for part of the observed variance. We were able
174 to obtain 6 GAS isolates from the blood cultures of these patients and analyzed the ability of
175 these strains to secrete EndoS into the culture medium *in vitro*. 3 isolates from severe sepsis
176 patients and 3 from septic shock patients (Fig. 3c, patients 1, 2 and 3) could be obtained. The
177 strains exhibited a large variability in EndoS expression as well as different levels of
178 degradation of the EndoS protein. Strains secreting substantial amounts of EndoS and strains
179 secreting almost no EndoS could be found in both groups. However, the amount of EndoS
180 secreted by the isolates from the septic shock patients *in vitro* corresponded well with the
181 amount of glycan-hydrolyzed IgG found in the corresponding patient´s blood plasma. The
182 isolate from the patient with no detectable IgG glycan hydrolysis *in vivo* did not secrete
183 detectable amounts of EndoS *in vitro,* and conversely, the isolate from the patient with the
184 highest *in vivo* glycan hydrolysis secreted the most EndoS *in vitro*. The cysteine protease
185 SpeB is a secreted GAS virulence factor and has been shown to cleave the EndoS enzyme[39].
186 Strikingly, SpeB is absent from the culture supernatant of the GAS isolate from patient 3
187 (with the highest degree of plasma IgG glycan hydrolysis, Fig. 3b) and consequently EndoS
188 is largely intact.

189 The IgG glycan hydrolysis we observed in plasma reflects a systemic modification of IgG,
190 which, due to the abundance of the antibody in circulation, necessitates large amounts of IgG
191 to be deglycosylated to reach detectable levels. Locally, at site of infection, the effects of

bioRxiv preprint doi: https://doi.org/10.1101/544064; this version posted February 13, 2019. The copyright holder for this preprint (which was not certified by peer review) is the author/funder, who has granted bioRxiv a license to display the preprint in perpetuity. It is made available under aCC-BY-NC-ND 4.0 International license.

EndoS on the IgG pool are likely to be much more pronounced. To test this, we obtained wound swabs from the infected tissue taken during surgery from two of the sepsis patients suffering from necrotizing fasciitis (patients 1 & 2). We analyzed them by SRM mass spectrometry to determine the degree of IgG glycan hydrolysis and compared the results to those previously obtained from analysis of plasma samples (Fig. 3d). The samples originated from two of the patients whose GAS isolates we have analyzed for EndoS expression *in vitro* (Fig. 3c, patients 1 & 2). One isolate did not secrete any detectable amounts (Fig. 3c, patient 1) whereas the other one exhibited high EndoS expression (Fig. 3c, patient 2). Accordingly, two very different patterns of IgG glycan hydrolysis could be observed in these patients (Fig 3d). The first patient showed no detectable IgG glycan hydrolysis in plasma and only a minor amount in the wound swab sample. The second patient on the other hand exhibited moderate IgG glycan hydrolysis in plasma (~0.7 % hydrolyzed) and the amount of IgG_{GH} was considerably higher in the wound swab sample from the same day (~30% hydrolyzed). This was no longer detectable in a sample from the same site that was taken during a second surgery the day after.

As we observed that local IgG glycan hydrolysis was transient, we wanted to determine how long-lasting the EndoS-mediated perturbation of the systemic IgG pool was. To this end we obtained further plasma samples taken throughout the treatment and recovery periods (until 12 days after admission) from the patient exhibiting the highest amount of IgG_{GH} in plasma (Fig. 3b, patient 3). Shortly after admission (time point 2h), the patient presented with very low total IgG levels (3.3 mg/ml) and a high degree of IgG glycan hydrolysis (1 mg/ml). The patient was given intravenous immunoglobulin (IVIG) treatment, upon which the total IgG levels quickly normalized but the concentration of IgG_{GH} stayed high throughout the analyzed time interval and was still around 0.5 mg/ml at the 12 days end point (Fig. 3e).

Taken together, these results show that EndoS is expressed and active during acute GAS infection *in vivo*. It is able to hydrolyze the glycans from a considerable portion of the IgG pool locally at the site of infection (both in tonsillitis and necrotizing fasciitis) as well as systemically in the most severe cases of GAS sepsis. This points towards an important role for EndoS in evasion of the immune defenses by perturbation of the hosts IgG response.

bioRxiv preprint doi: https://doi.org/10.1101/544064; this version posted February 13, 2019. The copyright holder for this preprint (which was not certified by peer review) is the author/funder, who has granted bioRxiv a license to display the preprint in perpetuity. It is made available under aCC-BY-NC-ND 4.0 International license.

EndoS is expressed during growth in saliva and protects GAS from phagocytic killing

While we were able to show that substantial IgG glycan hydrolysis takes place during GAS infections, the functional consequences of this process for GAS pathogenesis remained unclear and needed to be studied using appropriate model systems. As EndoS activity was measureable in the majority of samples from GAS tonsillitis patients, we attempted to set up a simplified *in vitro* model reminiscent of the conditions GAS encounters on an inflamed tonsil during such an infection. When GAS colonizes the throat it would encounter saliva, an increasing amount of plasma proteins as inflammation leads to vascular leakage[37] and finally phagocytic immune cells trying to eradicate the bacteria. To approximate these conditions, we grew GAS strains 5448 and AP1 as well as their respective isogenic *ndoS* mutants in sterile-filtered saliva supplemented with 5% serum and tested if EndoS would be expressed and active by SDS-PAGE. Based on electrophoretic mobility and/or LCA reactivity, both wild type strains but neither of the mutants were able to fully deglycosylate the IgG pool under these conditions (Fig. 4a, Fig. S6). Strain AP1 further expressed IdeS[11] leading to proteolytic cleavage of IgG hinge in the culture supernatant. This resulted in a population of antibodies where the Fc glycans and at least one half of the heavy chains had been cleaved (Fig. S6).

As IdeS and EndoS might be partially redundant and strain 5448 only secreted EndoS without any detectable IdeS activity when grown in saliva, we used this strain to test the resistance of wild type and *ndoS* mutant bacteria to phagocytic killing by human monocyte-derived macrophages (MDMs) and human polymorphonucelar leukocytes (PMNs) under the conditions described above. Deletion of the *ndoS* gene led to a small but significant increase in killing of the bacteria by both MDMs and PMNs (Fig. 4bc) and addition of recombinant EndoS reversed the phenotype. However, increased susceptibility to phagocytic killing was only observed when the assay was performed in the presence of serum containing GAS-specific IgGs (as determined by measuring the IgG response to streptococcal M1 protein by ELISA (Fig. S5)). In the absence of specific IgGs both mutant and wild type exhibited similar resistance to phagocytic killing. This indicates that EndoS confers increased resistance by neutralizing specific IgGs directed towards the pathogen and prevents them from mediating phagocytosis.

bioRxiv preprint doi: https://doi.org/10.1101/544064; this version posted February 13, 2019. The copyright holder for this preprint (which was not certified by peer review) is the author/funder, who has granted bioRxiv a license to display the preprint in perpetuity. It is made available under aCC-BY-NC-ND 4.0 International license.

252 ENDOS MUTANT GAS ARE LESS VIRULENT IN A MOUSE MODEL OF INVASIVE GAS INFECTION

253 In order to study the role of EndoS in neutralization of GAS-specific IgGs in more detail and
254 determine its contribution to the outcome of streptococcal infection, we established a mouse
255 model. As IdeS has no discernible activity on relevant subclasses of murine IgG (IgG1 and
256 IgG2b)[40] we were able to use the more mouse-virulent strain AP1 for these experiments
257 without confounding the results. Wild type and *ndoS* mutant[34] GAS were used to infect
258 C57BL/6J mice subcutaneously and both local (skin) and systemic (plasma, spleen) samples
259 were taken at 48h post infection to determine bacterial loads as well as IgG glycan hydrolysis
260 by SRM mass spectrometry (Fig. 5a). An assay analogous to the one for human IgGs was
261 developed to quantify murine IgG1 levels and its glycosylation status (Fig. S5). As EndoS
262 does not exhibit any murine IgG subclass specificity[41], this can be used as an indicator for
263 overall IgG glycan hydrolysis. When mice were infected with a wild type GAS strain, IgG1
264 was almost completely deglycosylated locally and around 30% glycan hydrolysis was
265 observed systemically (Fig. 5b, S8). The animals exhibited a heterogeneous response to
266 infection, with greatly varying degrees of severity observed. Consequently the measured
267 levels of IgG glycan hydrolysis also showed a large variance. We therefore tried to correlate
268 IgG glycan hydrolysis and bacterial load in the skin samples and found almost perfect
269 correlation (Fig. S5). Mice infected with the *ndoS* mutant developed local and systemic signs
270 of infection to a similar degree but showed no detectable IgG glycan hydrolysis (Fig. 5b,
271 S7,8). This indicates that EndoS is expressed and active during such an infection but does not
272 confer any selective advantages under these naïve conditions.

273 As EndoS targets the adaptive immune response, its functional role during GAS infection is
274 most appropriately studied in the context of adaptive immunity. We therefore immunized
275 mice prior to infection through two injections with purified streptococcal M1 protein
276 combined with adjuvant. After an IgG response to M1 was confirmed, the mice were infected
277 subcutaneously and survival was monitored for 5 days (Fig. 5c). This immunization protocol
278 lead to a complete protection at an infectious dose of 2.5×10^5 cfu which could be overcome
279 by increasing the dose to 2×10^7 cfu (Fig. S9). The majority of mice infected with wild type
280 bacteria at that dose succumbed to the infection within 2-3 days. On the other hand, more
281 than 90% of the mice infected with *ndoS* mutant bacteria survived the infection with only
282 milder symptoms (Fig 5d, left). This profound difference in susceptibility to infection
283 between wild-type and mutant could not be observed in animals that were mock immunized

bioRxiv preprint doi: https://doi.org/10.1101/544064; this version posted February 13, 2019. The copyright holder for this preprint (which was not certified by peer review) is the author/funder, who has granted bioRxiv a license to display the preprint in perpetuity. It is made available under aCC-BY-NC-ND 4.0 International license.

by injection of adjuvant only, where both groups showed a similarly high mortality (>90%, Fig. 5d, right).

Discussion

IgG is a central molecule of the mammalian immune system. It provides a link between adaptive and innate immunity by specifically binding to antigens presented by a pathogen with its Fab regions and recruiting immune effectors with its Fc region. Which exact effector functions are elicited is a highly regulated process that lets the immune system tune its response to the pathogen in question and mediate different effector functions against for example a gram-positive bacterium, a gram-negative bacterium or a virus. One determining factor in this process is the nature of the IgG antibody itself; namely its subclass and the structure of its Fc glycosylation.

We here present the first evidence of a pathogen exploiting this regulatory mechanism by specifically altering IgG Fc glycosylation *in vivo* during the clinical course of an infection. By implementing a targeted proteomics approach based on SRM-MS we were able to study the effects of EndoS on IgG antibodies during natural infections in human patients. Using SRM we were able to detect and absolutely quantify glycan-hydrolyzed IgGs in a subclass specific manner directly from a variety of very complex patient samples. With only minimal amounts of sample required and detection limits below 0.5 ng, this method is far superior to any other techniques used to measure IgG glycan hydrolysis to date. With this, we were able to quantitatively address the effects of EndoS on a patient IgG population during streptococcal infections. While a slight preference of EndoS towards IgG1[42] has been reported, we did not observe any subclass specificity in any of the patient samples (Table S4,5). Locally, at the site of infection, the degree of IgG glycan hydrolysis was generally high (up to nearly complete hydrolysis) but the effects were only transient, disappearing quickly upon therapeutic intervention. This was true both for mild infections (tonsillitis) as well as severe, invasive infections (necrotizing fasciitis). This indicates that at site of infection, IgG is turned over quickly and constantly replenished from the circulation and IgG glycan hydrolysis is only detectable as long as bacterial load is high and EndoS is continuously secreted. Due to the much larger amount of IgG in circulation as compared to the infected tissue and the increased dilution of the enzyme further away from the site of infection, effects on the systemic IgG pool in circulation were much harder to detect and therefore rarer. Only in the most severe cases of invasive infections (septic shock), could glycan hydrolysis be

bioRxiv preprint doi: https://doi.org/10.1101/544064; this version posted February 13, 2019. The copyright holder for this preprint (which was not certified by peer review) is the author/funder, who has granted bioRxiv a license to display the preprint in perpetuity. It is made available under aCC-BY-NC-ND 4.0 International license.

observed systemically. This systemic IgG glycan hydrolysis was long lasting with approximately half of the glycan-hydrolyzed IgGs still present after 12 days. A similarly slow recovery of IgG glycosylation to normal levels was also observed when rabbits or mice were injected with recombinant EndoS as an experimental treatment of autoimmunity[31,43].

In both of our patient sets, only a portion of the patient samples showed detectable levels of IgG_{GH} (58% of tonsillitis patients locally and 28% of sepsis patients systemically). In part, this might be due to some GAS isolates expressing only very low levels of EndoS (Fig. 3c). *In vivo* glycan hydrolysis was not associated with *covRS* mutation or any specific *emm*-type. Indeed we detected it in infections with at least different 8 different *emm*-types (Table S4,5). All publicly available GAS genome sequences contain an *ndoS* or an *ndoS*-like gene[44], but expression of the EndoS protein differs greatly between different GAS isolates. However, the fact that IgG glycan hydrolysis correlates to disease severity both in tonsillitis and invasive disease indicates that we – due to analytical limitations – might not be able to detect EndoS-mediated IgG glycan hydrolysis in samples from patients suffering from less severe infections. This is true especially for the GAS sepsis patient samples. Apart from two exceptions, we were only able to study IgG in blood plasma and therefore were unable to address potential perturbations of the local IgG pool at site of infection in more detail. Indeed among the sickest patients in each cohort the percentage of samples with detectable IgG_{GH} was considerably higher. 5 out of 6 GAS septic shock patients (83%) exhibited measureable systemic IgG glycan hydrolysis and among the sickest half of the tonsillitis patients (based on estimation of general malaise) glycan hydrolysis of the local IgG pool was detectable in all but one patient (92% total). While studying the activity of EndoS during GAS tonsillitis, we also observed a considerable amount of IgG glycan hydrolysis in some of our control samples. We speculate that this was due to enzymatic activities of the oral micro flora, especially oral streptococci which are known to express a large number of glycoside hydrolases[45]. This is supported by the fact that IgG glycan hydrolysis was not detectable in any of the samples we took after antibiotic treatment.

While we were able to show that IgG glycan hydrolysis takes place during GAS infection *in vivo*, the functional consequences of this process could not be deduced directly from the patient data. Removal of the Fc glycan by EndoS has previously been shown to impair both Fc receptor interaction and complement activation *in vitro*[20,25]. While EndoS has been speculated to contribute to GAS virulence, all studies showing this to date had to resort either to addition of recombinant EndoS or overexpression[25,26] to see any effect. Thus, the

bioRxiv preprint doi: https://doi.org/10.1101/544064; this version posted February 13, 2019. The copyright holder for this preprint (which was not certified by peer review) is the author/funder, who has granted bioRxiv a license to display the preprint in perpetuity. It is made available under aCC-BY-NC-ND 4.0 International license.

349 conditions under which endogenous EndoS is expressed, active and able to confer a selective
350 advantage to the bacteria remained unclear. EndoS expression is highly regulated and while
351 the regulatory network responsible remains obscured, it has been shown to involve both
352 transcriptional regulation by *ccpA* and weakly by *covR/S*[46] as well as posttranslational
353 regulation through proteolysis[47]. Transcriptomics studies have shown that EndoS expression
354 is repressed during growth in rich medium[48] (such as the standard Todd-Hewitt broth) and is
355 not induced until the bacteria reach stationary phase[49]. This means that most standard assays
356 used to study streptococcal virulence factors such as incubating log phase bacteria with
357 phagocytic cells and IgG (or the classic Lancefield assay[50]) are ill suited to address the role of
358 EndoS or similar secreted immunomodulatory activities. This might constitute a major
359 shortcoming in for example analysis of protective effects of IgGs in vaccination studies,
360 potentially resulting in overestimation of vaccine efficacy.

361 We used our characterization of IgG glycan hydrolysis *in vivo* to set up relevant model
362 systems to address the contribution of EndoS to GAS pathogenesis. Based on our findings on
363 IgG glycan hydrolysis during GAS tonsillitis, we were able to approximate the conditions
364 GAS encounters on an inflamed tonsil using human saliva and serum. This prompted wild
365 type bacteria to secrete enough EndoS to completely deglycosylate the IgGs present and
366 neutralize the contribution of GAS-specific IgGs to phagocytic killing by human
367 macrophages or neutrophils *in vitro*. *ndoS* mutant bacteria on the other hand were unable to
368 cleave the glycans from IgG and consequently exhibited a higher susceptibility to phagocytic
369 killing. This phenotype could be reversed by externally adding recombinant EndoS. These
370 results, together with the fact that the *ndoS* mutation had no phenotype in the absence of
371 GAS-specific IgGs indicates that the observed phenotype is due to deglycosylation of the
372 GAS-specific IgGs which in turn impairs their ability to mediate phagocytic killing. There
373 seems to be no general attenuation of the *ndoS* mutant, nor any benefits in glycan hydrolysis
374 of non-specific IgGs.

375 An animal model of local skin infection leading to invasive infection showed very similar
376 dynamics. Mice infected with *ndoS* mutant bacteria exhibited no IgG glycan hydrolysis and
377 were significantly less likely to die from the infection than mice infected with wild type GAS.
378 This difference was however only clearly evident in the context of adaptive immunity (i.e. in
379 animals that had been immunized against GAS prior to infection). In agreement with the
380 results from the phagocytosis assays and previous studies[26], naïve mice showed a very similar
381 susceptibility towards both wild type and *ndoS* mutant bacteria; with no significant

bioRxiv preprint doi: https://doi.org/10.1101/544064; this version posted February 13, 2019. The copyright holder for this preprint (which was not certified by peer review) is the author/funder, who has granted bioRxiv a license to display the preprint in perpetuity. It is made available under aCC-BY-NC-ND 4.0 International license.

differences in survival, weight loss or bacterial load in the skin (Fig. 5, Fig. S7). Only the bacterial burden in the spleen was slightly decreased in mice infected with *ndoS* mutant bacteria (Fig. S7). This might point to a small degree of innate protection conferred by natural IgGs[51] that can be counteracted by EndoS.

While not generally used to treat sepsis[52,53], administration of intravenous immunoglobulin (IVIG) has shown promise as a treatment for streptococcal toxic shock syndrome[54,55] and necrotizing fasciitis[56]. Its mode of action is thought to involve neutralization of bacterial superantigens and inhibition of pro-inflammatory signaling[57-59]. Our data points to another reason why IVIG treatment could improve the outcome of severe streptococcal infections. EndoS-mediated glycan hydrolysis inactivates IgGs and as shown in this study, such antibody modifications can be systemic, long lasting and affect a considerable fraction of the patient's total IgG pool. GAS can lower functional IgG levels even further through secretion of the IgG protease IdeS[11,37]. In such cases, IVIG in concert with antimicrobial therapy could help to quickly normalize the level of functional IgG in circulation. We observed such an effect in one patient (Fig. 3e, patient 3).

Despite an abundance of anti-GAS IgGs in the serum of most people[4-7], protective immunity towards the pathogen does not ensue. Furthermore, development of effective GAS vaccines has proven challenging. Herein we present a possible mechanism to explain why anti-GAS IgGs often confer such poor protection: GAS is able to effectively neutralize the contribution of IgG to host defense through specific degradation of the IgG antibodies. We have demonstrated the dynamics of IgG glycan hydrolysis by EndoS in this study and a recent study has also shown significant levels of IdeS-mediated IgG proteolysis during GAS infections *in vivo*[37]. This makes GAS a very proficient evader of IgG-mediated immunity, a fact that has implications for the treatment of severe GAS infections and has to be taken into account in future research into the immune response to GAS as well as in the continuing efforts at development of an effective vaccine against the pathogen. Finally, immune evasion through modification of IgG glycosylation might not be restricted to GAS and enzymes similar to EndoS can be found in many other pathogenic species such as *Enterococcus faecalis*[60], *Streptococcus pneumoniae*[61] as well as other non-group A streptococci[62,63]. Indeed, an EndoS homolog from *Streptococcus equi*[63] proved a protective antigen in a vaccination trial in mice, pointing towards its importance for the infection process. Bacterial modulation of IgG glycosylation might therefore be a more widespread phenomenon that warrants further study.

bioRxiv preprint doi: https://doi.org/10.1101/544064; this version posted February 13, 2019. The copyright holder for this preprint (which was not certified by peer review) is the author/funder, who has granted bioRxiv a license to display the preprint in perpetuity. It is made available under aCC-BY-NC-ND 4.0 International license.

Materials and Methods

Patient samples

Tonsillar swabs (n = 54, ESwab Liquid Amies) were obtained from patients (>8 years old) seeking clinical care because of a sore throat at the primary healthcare clinics at Laurentiikliniken and Skåne University Hospital (SUS) both in Lund, Sweden. GAS tonsillitis was diagnosed by rapid strep test (antigen detection) and routine bacterial culturing. A follow-up tonsillar swab sample (3-5 days post) was taken from a subset of patients (n=5) treated with antibiotics (Table S4). Wound swabs from the local infection site of patients clinically diagnosed with GAS sepsis and necrotizing fasciitis were obtained from SUS, Lund Sweden (n=4) during surgical intensive care (Table S5). Patient swab samples were transported on dry ice before storage at -80 °C. The patient plasma samples were part of a larger cohort collected at the Clinic for Infectious Diseases or at Intensive Care Unit at Lund University Hospital between 2005 and 2015. All human samples were obtained with informed consent and with the approval of the local ethics committee (see 'Ethical Considerations' section below).

Sample preparation for mass spectrometry

Proteins from the swab samples were extracted and homogenized in water using a bead-beater (Fastprep-96, MP-Biomedicals). 0.625 µl plasma or 50 µg of protein from swabs or skin homogenates were prepared for MS analysis using the SmartDigest Kit (Thermo Scientific). Samples were denatured at 90°C followed by digestion for 3.5 hours at 70°C. The peptides were reduced using 50 mM TCEP, alkylated with 100 mM iodoacetamide and finally purified using SOLAµ HRP plates (Thermo Scientific). The peptide samples were dried in a vacuum centrifuge and dissolved in 100 µl 50 mM sodium acetate buffer (pH 5) containing 50 mU Thermatoga maritima α-fucosidase (Megazymes). After incubation at 70°C for 14 h, the samples were purified a second time on SOLAµ HRP plates and dried in a vacuum centrifuge.

SRM mass spectrometry

Peptide samples were dissolved in 2%ACN, 0.2% FA and AQUA peptides (Thermo HeavyPeptide QuantPro, table S3) were spiked in. The amount of peptide standards was adjusted so that the ratio of light to heavy signal falls within the interval of 0.1 to 10. Sample corresponding to 1 µg of protein were analyzed by SRM mass spectrometry using a TSQ Vantage triple quadrupole mass spectrometer coupled to an Easy-nLC II system (both

bioRxiv preprint doi: https://doi.org/10.1101/544064; this version posted February 13, 2019. The copyright holder for this preprint (which was not certified by peer review) is the author/funder, who has granted bioRxiv a license to display the preprint in perpetuity. It is made available under aCC-BY-NC-ND 4.0 International license.

Thermo Scientific) equipped with a PicoChip column (PCH7515-105H354-FS25, New Objective). Data was acquired with a spray voltage of 1500V, 0.7 FWHM on both quadrupoles and a dwell time of 10ms. Assays for all the non-glycopeptides were obtained from published studies [37,64] while glycopeptide assays were developed as described here[65]. Assay set-up, empirical collision energy optimization as well as data analysis was done using Skyline [66,67]. The analyzed transitions are listed in table S2.

DETERMINATION OF DETECTION LIMITS

Human IgG subclass reference serum NOR-1 (NordicMUBio) was used to create standard samples for method calibration and determination of detection limits. For a fully glycan hydrolyzed sample, the serum was incubated with 50 µg/ml recombinant EndoS at 37°C for 16h. Both treated and untreated serum samples were prepared for mass spectrometry analysis separately as described above. Peptides were dissolved in 2%ACN, 0.2% FA at a concentration of 1 µg/µl and spiked with AQUA IgG glycopeptides. The EndoS-treated sample was further spiked with AQUA IgG peptides. Three separate dilution series were prepared by serially diluting the EndoS-treated sample with peptides from the untreated sample. Finally, peptides samples corresponding to 1 µg of protein form each dilution were analyzed by SRM mass spectrometry. From this data set detection limits for each peptide were determined separately:

Limit of blank (LoB): $LoB = mean_{blank} + 1.645(SD_{blank})$ (1)

Limit of detection (LoD): $LoD = (LoB + 1.645(SD_{low\ concentration\ sample})$ (2)

Untreated samples were used to determine LoB according to formula 1. The first dilution with a concentration above LoB was used as the low concentration sample for LoD determination with formula 2. A lower limit of quantification (LLoQ) was defined as two time LoD and in all further experiments, measured amounts below LLoQ were considered as being 0. As the concentrations of all 4 IgG subclasses in serum NOR-1 have been determined by the manufacturer, we could also use this dataset to calibrate the quantification and correct for incomplete digestion and sample loss during preparation. For each data point above LOD and with a light to heavy between 0.1 and 10 conversion factors were determined by dividing the known IgG subclass concentrations with the measured light to heavy ratios. These conversion factors were averaged (table S3) and are used to determine absolute amounts from measured light to heavy ratios in all further experiments with human samples. The same procedure was followed when the assay for murine IgG1 was developed. The standard

bioRxiv preprint doi: https://doi.org/10.1101/544064; this version posted February 13, 2019. The copyright holder for this preprint (which was not certified by peer review) is the author/funder, who has granted bioRxiv a license to display the preprint in perpetuity. It is made available under aCC-BY-NC-ND 4.0 International license.

479 sample there was a monoclonal mouse IgG1 (MA-69, Biolegend, San Diego, USA) that was
480 treated with recombinant EndoS and spiked into human plasma as a background proteome.

481 SDS-PAGE AND LECTIN BLOT

482 IgG was purified using Protein G (Ab SpinTrap, GE Healthcare). Samples were separated on
483 SDS-PAGE (Mini-protean TGX stainfree gels, 4-15% acrylamide, BioRad), imaged using a
484 ChemiDoc MP imaging system (BioRad) and transferred to low fluorescent PVDF
485 membranes using the Transblot Turbo kit (BioRad). Membranes were blocked for 1h in lectin
486 buffer (10 mM HEPES pH7.5, 150 mM NaCl, 0.01 mM $MnCl_2$, 0.1 mM $CaCl_2$, 0.1% (v/v)
487 tween 20) followed by incubation with 5 µg/ml fluorescein-labeled LCA lectin (Vector
488 laboratories). After extensive washing in lectin buffer, the membranes were imaged using a
489 ChemiDoc MP imaging system (BioRad).

490 ANALYSIS OF ENDOS AND SPEB EXPRESSION *IN VITRO*

491 AP1, AP1ΔndoS, AP1ΔspeB and the GAS clinical isolates were grown overnight at 37°C,
492 5% CO_2 in C-medium (0.5% (w/v) Proteose Peptone No. 2 (Difco) and 1.5% (w/v) yeast
493 extract (Oxoid) dissolved in CM buffer (10 mM K_2PO_4, 0.4 mM $MgSO_4$, 17 mM NaCl
494 pH 7.5). The cultures were pelleted and the supernatants sterile filtered (Millex-GP filter unit
495 0.22µm, Millipore). Proteins were precipitated from the supernatants with 5% TCA
496 (trichloroacetic acid) and analyzed by SDS-PAGE under reducing conditions. Proteins were
497 transferred to PVDF-membranes using the Trans-Blot Turbo equipment (Bio-Rad
498 Laboratories) according to manufacturer's instructions. Membranes were blocked with 5%
499 (w/v) blotting-grade blocker (Bio-Rad Laboratories) in PBST, followed by incubation with
500 EndoS or SpeB rabbit antiserum [12,68] another wash and incubation with a secondary antibody
501 (goat anti-rabbit HRP-conjugated antibody, BioRad). The membranes were developed using
502 Clarity Western ECL substrate (BioRad) and visualized with a ChemiDoc MP Imager (Bio-
503 Rad, USA).

504 ANALYSIS OF *EMM* AND *COVRS* SEQUENCES

505 *emm* sequences of the GAS clinical isolates were analyzed according to protocols published
506 by the CDC and compared to a database of known *emm* sequences using the tool on the CDC
507 website (https://www2a.cdc.gov/ncidod/biotech/strepblast.asp). The *covRS* operon was
508 sequenced as previously described[69] and compared to published sequences of the same
509 serotype.

bioRxiv preprint doi: https://doi.org/10.1101/544064; this version posted February 13, 2019. The copyright holder for this preprint (which was not certified by peer review) is the author/funder, who has granted bioRxiv a license to display the preprint in perpetuity. It is made available under aCC-BY-NC-ND 4.0 International license.

IN VITRO TONSILLITIS MODEL

Preparation of saliva: Saliva from healthy volunteers was collected in the morning after extensive brushing of the teeth. The saliva was centrifuged (20 min, 20000 g), sterile filtered (Steriflip GP 0.22 µm, Milipore) and either used directly or kept at -20°C until use.

Preparation of polymorphonuclear leukocytes (PMNs): 20 ml blood was collected into EDTA blood collection tubes (BD Bioscience) and the PMNs were isolated using PolyMorphPrep (Axis-shield) according to manufacturers recommendations. After counting, the cells were diluted into RPMI medium and seeded at 50000 cells/well into a 96-well plate.

Preparation of monocyte derived macrophages (MDMs):

Peripheral blood mononuclear cells (PBMCs) were isolated from leukocytes of healthy anonymous donors provided by the Lund University Hospital. Red blood cells were removed by centrifugation on Lymphoprep (Fresenius Norge As, Oslo, Norway) and recovered PBMCs were washed to remove platelets. Monocytes were isolated using a magnetic cell separation system with anti-CD14 mAb-coated microbeads (Miltenyi Biotec). CD14-positive monocytes were seeded into 12 well plates at 5×10^5 cells/well and differentiated into macrophages by culture in complete RPMI 1640 medium (Gibco) supplemented with 10% heat-inactivated human AB+ serum, 50 nM β-mercaptoethanol (GIBCO), Penicillin-Streptomycin (Sigma) and 40 ng/ml M-CSF (Peprotech) at 37°C under a humidified 5% CO2 atmosphere for 6 days. Medium was replaced on day 2 and on day 4, when cells were washed with PBS and the medium was replaced with antibiotic-fee medium. The cells were further incubated until day 6 when the infection experiments took place.

Killing assays: GAS 5448 and an isogenic *ndoS* mutant[26] were grown overnight in THY medium at 37°C, 5% CO_2, diluted 1:10 into fresh medium and let grow to mid-log phase (OD = 0.4). Cultures were diluted 1:50 into 1 ml of saliva, incubated for 2h at 37°C, 5% CO_2 and diluted again (1:20) into 1 ml fresh saliva (supplemented with 5% serum and 0.5 µg/ml recombinant EndoS where suitable). After 20h at 37°C, 5% CO_2 the bacteria were diluted 1:10 into RPMI medium and used to infect PMNs or MDMs at an MOI of 2. After 30min (for PMNs) or 2 h (for MDMs) incubation at 37°C, 5% CO_2 the cells were lysed using ddH2O (for PMNs) or 0.025% Triton X-100 (for MDMs) and the number of surviving bacteria was determined by plating on THY agar plates.

bioRxiv preprint doi: https://doi.org/10.1101/544064; this version posted February 13, 2019. The copyright holder for this preprint (which was not certified by peer review) is the author/funder, who has granted bioRxiv a license to display the preprint in perpetuity. It is made available under aCC-BY-NC-ND 4.0 International license.

540 ANALYSIS OF ENDOS EXPRESSION *IN VITRO*

541 AP1, the *ndoS* mutant and the GAS clinical isolates were grown in C-medium (37°C and 5%
542 CO2) overnight and normalized to the same OD_{620} using fresh C-medium. Bacteria were
543 pelleted by centrifugation and the supernatants filtered (Millex-GP filter unit 0.22µm,
544 Millipore). Proteins were precipitated from the supernatants with 5% TCA (trichloroacetic
545 acid) and analyzed by SDS-PAGE under reducing conditions. Proteins were transferred to
546 PVDF-membranes using the Trans-Blot Turbo kit (Bio-Rad Laboratories) according to
547 manufacturer's instructions. Membranes were blocked with 5% (w/v) blotting-grade blocker
548 (Bio-Rad Laboratories) in PBST, followed by incubation with EndoS[34] or SpeB[68] antiserum
549 The membranes were washed followed by incubation with a secondary antibody (goat anti-
550 rabbit HRP-conjugated antibody, BioRad). The membranes were developed using Clarity
551 Western ECL substrate (BioRad) and visualized with a ChemiDoc MP Imager (Bio-Rad,
552 USA).

553 MOUSE INFECTIONS:

554 *Acute infection model of GAS in naïve C57BL/6J mice* GAS AP1 and *ndoS* mutant (Table S1)
555 were grown to logarithmic phase in Todd–Hewitt broth (37°C, 5% CO_2). Bacteria were
556 washed and resuspended in sterile PBS. 2-3x10^5 cfu of AP1 (n=13) or *ndoS* mutant (n=13)
557 were injected subcutaneously into the flank of 9-week-old female C57BL/6J mice (Scanbur/
558 Charles River Laboratories). Control mice were injected with PBS (n=8). Mice were
559 rehydrated subcutaneously with saline at 24 h post infection. Body weight and general
560 symptoms of infection were monitored regularly. Mice were sacrificed at 48 h post infection
561 and organs (blood, spleens and skin) were harvested to determine the degree of bacterial
562 dissemination and IgG glycan hydrolysis.

563 *M1 immunization and survival study* 9-week-old female C57BL/6J mice (Scanbur/ Charles
564 River Laboratories) were injected subcutaneously with M1 protein on days 0 and 21 (10
565 µg/dose), purified as previously described[68,71]. The protein was administered as a 50:50
566 solution of M1:adjuvant (TiterMax Gold), in a 50 µl volume. Control mice were similarly
567 injected with PBS:adjuvant solution. Serum was collected at day 49 and anti-M1 titers were
568 measured by ELISA as previously described[72] with a goat anti-mouse HRP-conjugated
569 secondary antibody at 1:5000 (BioRad). Immunized and control mice were infected
570 subcutaneously into the flank with 2x10^7 cfu of the AP1 (n=17) or *ndoS* mutant (n=12) at day
571 56. Mice were rehydrated subcutaneously with saline 24 h post infection. Weight and general

bioRxiv preprint doi: https://doi.org/10.1101/544064; this version posted February 13, 2019. The copyright holder for this preprint (which was not certified by peer review) is the author/funder, who has granted bioRxiv a license to display the preprint in perpetuity. It is made available under aCC-BY-NC-ND 4.0 International license.

symptoms of infection were monitored every 12 h during the acute phase of the infection, and then every 24 h until termination of the study at 5 days post infection. Animals displaying a weight loss exceeding 20% (until 72 h post infection) or 15% (after 72 h post infection) were considered moribund and sacrificed.

Statistics

All statistical analyses were preformed using GraphPad Prism 7. Phagocytic killing assays were analyzed using one-way ANOVA followed by Tukey´s multiple comparison test. IgG hydrolysis data was analyzed using a Mann-Whitney test or a Kruskal-Wallis test in combination with Dunn´s multiple comparison test (when more than two datasets were compared). Correlation was determined according to Spearman and survival data was analyzed using a Mantle-Cox test.

Ethical considerations

All animal use and procedures were approved by the local Malmö/Lund Institutional Animal Care and Use Committee, ethical permit number M115-13. Collection and analysis of human throat swabs and plasma samples was approved by the local ethics committee (dnr 2005/790, 2015/314 and 2016/39).

Author contributions

AN designed the study, performed all mass spectrometry and phagocytosis experiments and wrote the manuscript. EB and OS designed and performed all animal experiments. CK helped with SRM assay development and data analysis. AL organized and supervised collection of clinical samples. RK prepared cells for phagocytosis experiments. JM and MC designed the study, supervised the research, and wrote the manuscript.

Data availability

The MS analysis files from Skyline underlying figures 1d, 2b, 3bde and 5b are available on PanoramaWeb (https://panoramaweb.org/endos.url). The MS raw data is available upon request.

Acknowledgements

We thank Fanny Olsson Byrlind and Tomas Lindgren for help with collection of patient samples, Bo Nilsson for collecting the GAS clinical isolates, and Fredric Carlsson for helpful discussions about the choice of animal model. This work was supported by grants to AN from the Swiss National Science Foundation (P2EZP3_155594 and P300PA_167754), the

bioRxiv preprint doi: https://doi.org/10.1101/544064; this version posted February 13, 2019. The copyright holder for this preprint (which was not certified by peer review) is the author/funder, who has granted bioRxiv a license to display the preprint in perpetuity. It is made available under aCC-BY-NC-ND 4.0 International license.

Royal Physiographic Society in Lund and the Sigurd and Elsa Goljes Memorial Foundation. This work was further supported by grants to MC from the Swedish Research Council (projects 2012-1875 and 2017-02147), the Royal Physiographic Society in Lund, the Foundations of Åke Wiberg, Alfred Österlund, Gyllenstierna-Krapperup, Torsten Söderberg, the King Gustaf V`s 80 years fund, and Hansa Medical AB as well as grants to JM from Foundation of Knut and Alice Wallenberg (2016.0023), European research council starting grant (ERC-2012-StG-309831), the Swedish Research Council (project 2015-02481), the Wallenberg Academy Fellow program KAW (2012.0178 and 2017.0271), Olle Engkvist Byggmästare and the Medical Faculty of Lund University. The funders had no role in preparation of the manuscript or in the decision to publish

References

1. Walker, M. J. *et al.* Disease manifestations and pathogenic mechanisms of group a Streptococcus. *Clin. Microbiol. Rev.* **27,** 264–301 (2014).
2. Carapetis, J. R., Steer, A. C., Mulholland, E. K. & Weber, M. The global burden of group A streptococcal diseases. *Lancet Infect. Dis.* **5,** 685–694 (2005).
3. St Sauver, J. L., Weaver, A. L., Orvidas, L. J., Jacobson, R. M. & Jacobsen, S. J. Population-based prevalence of repeated group A beta-hemolytic streptococcal pharyngitis episodes. *Mayo Clin. Proc.* **81,** 1172–1176 (2006).
4. Lancefield, R. C. Current knowledge of type-specific M antigens of group A streptococci. *J. Immunol.* **89,** 307–313 (1962).
5. Todd, E. W. Antigenic Streptococcal hemolysin. *J. Exp. Med.* **55,** 267–280 (1932).
6. Åkesson, P. *et al.* Low antibody levels against cell wall-attached proteins of *Streptococcus pyogenes* predispose for severe invasive disease. *J. Infect. Dis.* **189,** 797–804 (2004).
7. O'Connor, S. P. *et al.* The human antibody response to streptococcal C5a peptidase. *J. Infect. Dis.* **163,** 109–116 (1991).
8. McMillan, D. J. *et al.* Updated model of group A Streptococcus M proteins based on a comprehensive worldwide study. *Clin. Microbiol. Rev.* **19,** E222–9 (2013).
9. Åkesson, P., Schmidt, K. H., Cooney, J. & Björck, L. M1 protein and protein H: IgGFc- and albumin-binding streptococcal surface proteins encoded by adjacent genes. *Biochem. J.* **300 (Pt 3),** 877–886 (1994).
10. Åkesson, P., Cooney, J., Kishimoto, F. & Björck, L. Protein H--a novel IgG binding bacterial protein. *Mol. Immunol.* **27,** 523–531 (1990).
11. Pawel-Rammingen, von, U., Johansson, B. P. & Björck, L. IdeS, a novel streptococcal cysteine proteinase with unique specificity for immunoglobulin G. *EMBO J* **21,** 1607–1615 (2002).
12. Collin, M. & Olsén, A. EndoS, a novel secreted protein from *Streptococcus pyogenes* with endoglycosidase activity on human IgG. *EMBO J* **20,** 3046–3055 (2001).
13. Subedi, G. P. & Barb, A. W. The structural role of antibody N-glycosylation in receptor interactions. *Structure* **23,** 1573–1583 (2015).
14. Subedi, G. P. & Barb, A. W. The immunoglobulin G1 N-glycan composition affects binding to each low affinity Fc γ receptor. *Mabs* **8,** 1512–1524 (2016).

bioRxiv preprint doi: https://doi.org/10.1101/544064; this version posted February 13, 2019. The copyright holder for this preprint (which was not certified by peer review) is the author/funder, who has granted bioRxiv a license to display the preprint in perpetuity. It is made available under aCC-BY-NC-ND 4.0 International license.

15. Burton, D. R. Immunoglobulin G: functional sites. *Mol. Immunol.* **22,** 161–206 (1985).
16. Burton, D. R. & Dwek, R. A. Immunology. Sugar determines antibody activity. *Science* **313,** 627–628 (2006).
17. Shinkawa, T. *et al.* The absence of fucose but not the presence of galactose or bisecting N-acetylglucosamine of human IgG1 complex-type oligosaccharides shows the critical role of enhancing antibody-dependent cellular cytotoxicity. *J. Biol. Chem.* **278,** 3466–3473 (2003).
18. Okazaki, A. *et al.* Fucose depletion from human IgG1 oligosaccharide enhances binding enthalpy and association rate between IgG1 and FcgammaRIIIa. *J. Mol. Biol.* **336,** 1239–1249 (2004).
19. Peschke, B., Keller, C. W., Weber, P., Quast, I. & Lünemann, J. D. Fc-galactosylation of human immunoglobulin gamma isotypes improves C1q binding and enhances complement-dependent cytotoxicity. *Front Immunol* **8,** 646 (2017).
20. Lux, A., Yu, X., Scanlan, C. N. & Nimmerjahn, F. Impact of immune complex size and glycosylation on IgG binding to human FcγRs. *J. Immunol.* **190,** 4315–4323 (2013).
21. Nose, M. & Wigzell, H. Biological significance of carbohydrate chains on monoclonal antibodies. *Proc. Natl. Acad. Sci. U.S.A.* **80,** 6632–6636 (1983).
22. Alter, G. *et al.* High-resolution definition of humoral immune response correlates of effective immunity against HIV. *Mol. Syst. Biol.* **14,** e7881 (2018).
23. Lu, L. L. *et al.* A Functional Role for Antibodies in Tuberculosis. *Cell* **167,** 433–443.e14 (2016).
24. Allhorn, M., Olin, A. I., Nimmerjahn, F. & Collin, M. Human IgG/Fc gamma R interactions are modulated by streptococcal IgG glycan hydrolysis. *PLoS ONE* **3,** e1413 (2008).
25. Collin, M. *et al.* EndoS and SpeB from *Streptococcus pyogenes* inhibit immunoglobulin-mediated opsonophagocytosis. *Infect. Immun.* **70,** 6646–6651 (2002).
26. Sjögren, J., Okumura, C. Y. M., Collin, M., Nizet, V. & Hollands, A. Study of the IgG endoglycosidase EndoS in group A streptococcal phagocyte resistance and virulence. *BMC Microbiol.* **11,** 120 (2011).
27. Picotti, P. & Aebersold, R. Selected reaction monitoring-based proteomics: workflows, potential, pitfalls and future directions. *Nat Meth* **9,** 555–566 (2012).
28. Anderson, L. & Hunter, C. L. Quantitative mass spectrometric multiple reaction monitoring assays for major plasma proteins. *Mol. Cell Proteomics* **5,** 573–588 (2006).
29. Addona, T. A. *et al.* Multi-site assessment of the precision and reproducibility of multiple reaction monitoring-based measurements of proteins in plasma. *Nat. Biotechnol.* **27,** 633–641 (2009).
30. Hong, Q., Lebrilla, C. B., Miyamoto, S. & Ruhaak, L. R. Absolute quantitation of immunoglobulin G and its glycoforms using multiple reaction monitoring. *Anal. Chem.* **85,** 8585–8593 (2013).
31. Collin, M., Shannon, O. & Björck, L. IgG glycan hydrolysis by a bacterial enzyme as a therapy against autoimmune conditions. *Proc. Natl. Acad. Sci. U.S.A.* **105,** 4265–4270 (2008).
32. Sjögren, J. *et al.* EndoS and EndoS2 hydrolyze Fc-glycans on therapeutic antibodies with different glycoform selectivity and can be used for rapid quantification of high-mannose glycans. *Glycobiology* **25,** 1053–1063 (2015).
33. Dixon, E. V. *et al.* Fragments of bacterial endoglycosidase s and immunoglobulin g reveal subdomains of each that contribute to deglycosylation. *J. Biol. Chem.* **289,** 13876–13889 (2014).
34. Collin, M. & Olsén, A. EndoS, a novel secreted protein from *Streptococcus pyogenes*

bioRxiv preprint doi: https://doi.org/10.1101/544064; this version posted February 13, 2019. The copyright holder for this preprint (which was not certified by peer review) is the author/funder, who has granted bioRxiv a license to display the preprint in perpetuity. It is made available under aCC-BY-NC-ND 4.0 International license.

with endoglycosidase activity on human IgG. *EMBO J* **20,** 3046–3055 (2001).

35. Pucić, M. *et al.* High throughput isolation and glycosylation analysis of IgG-variability and heritability of the IgG glycome in three isolated human populations. *Mol. Cell Proteomics* **10,** M111.010090 (2011).
36. Wuhrer, M. *et al.* Glycosylation profiling of immunoglobulin G (IgG) subclasses from human serum. *Proteomics* **7,** 4070–4081 (2007).
37. Karlsson, C. A. Q. *et al. Streptococcus pyogenes* infection and the human proteome with a special focus on the IgG-cleaving enzyme IdeS. *Mol. Cell Proteomics* mcp.RA117.000525 (2018). doi:10.1074/mcp.RA117.000525
38. Centor, R. M., Witherspoon, J. M., Dalton, H. P., Brody, C. E. & Link, K. The diagnosis of strep throat in adults in the emergency room. *Med. Decis. Making* **1,** 239–246 (1981).
39. Allhorn, M., Olsén, A. & Collin, M. EndoS from *Streptococcus pyogenes* is hydrolyzed by the cysteine proteinase SpeB and requires glutamic acid 235 and tryptophans for IgG glycan-hydrolyzing activity. *BMC Microbiol.* **8,** 3 (2008).
40. Nandakumar, K. S., Johansson, B. P., Björck, L. & Holmdahl, R. Blocking of experimental arthritis by cleavage of IgG antibodies in vivo. *Arthritis Rheum.* **56,** 3253–3260 (2007).
41. Albert, H., Collin, M., Dudziak, D., Ravetch, J. V. & Nimmerjahn, F. In vivo enzymatic modulation of IgG glycosylation inhibits autoimmune disease in an IgG subclass-dependent manner. *Proc. Natl. Acad. Sci. U.S.A.* **105,** 15005–15009 (2008).
42. Trastoy, B. *et al.* Crystal structure of *Streptococcus pyogenes* EndoS, an immunomodulatory endoglycosidase specific for human IgG antibodies. *Proc. Natl. Acad. Sci. U.S.A.* **111,** 6714–6719 (2014).
43. Benkhoucha, M. *et al.* IgG glycan hydrolysis by EndoS inhibits experimental autoimmune encephalomyelitis. *J. Neuroinflammation* **9,** 209 (2012).
44. Sjögren, J. *et al.* EndoS2 is a unique and conserved enzyme of serotype M49 group A *Streptococcus* that hydrolyses N-linked glycans on IgG and alpha1-acid glycoprotein. *Biochem. J.* **455,** 107–118 (2013).
45. Nord, C. E., Linder, L., Wadström, T. & Lindberg, A. A. Formation of glycoside-hydrolases by oral streptococci. *Arch. Oral Biol.* **18,** 391–402 (1973).
46. Shelburne, S. A. *et al.* A combination of independent transcriptional regulators shapes bacterial virulence gene expression during infection. *PLoS Pathog* **6,** e1000817 (2010).
47. Collin, M. & Olsén, A. Effect of SpeB and EndoS from *Streptococcus pyogenes* on human immunoglobulins. *Infect. Immun.* **69,** 7187–7189 (2001).
48. Shelburne, S. A. *et al.* A direct link between carbohydrate utilization and virulence in the major human pathogen group A *Streptococcus*. *Proc. Natl. Acad. Sci. U.S.A.* **105,** 1698–1703 (2008).
49. Bao, Y.-J. *et al.* CovRS-regulated transcriptome analysis of a hypervirulent M23 strain of group A *Streptococcus pyogenes* provides new insights into virulence determinants. *J. Bacteriol.* **197,** 3191–3205 (2015).
50. Lancefield, R. C. Differentiation of group A streptococci with a common R antigen into three serological types, with special reference to the bactericidal test. *J. Exp. Med.* **106,** 525–544 (1957).
51. Panda, S., Zhang, J., Tan, N. S., Ho, B. & Ding, J. L. Natural IgG antibodies provide innate protection against ficolin-opsonized bacteria. *EMBO J* **32,** 2905–2919 (2013).
52. Norrby-Teglund, A., Ihendyane, N. & Darenberg, J. Intravenous immunoglobulin adjunctive therapy in sepsis, with special emphasis on severe invasive group A streptococcal infections. *Scand. J. Infect. Dis.* **35,** 683–689 (2003).
53. Alejandria, M. M., Lansang, M. A. D., Dans, L. F. & Mantaring, J. B. Intravenous

bioRxiv preprint doi: https://doi.org/10.1101/544064; this version posted February 13, 2019. The copyright holder for this preprint (which was not certified by peer review) is the author/funder, who has granted bioRxiv a license to display the preprint in perpetuity. It is made available under aCC-BY-NC-ND 4.0 International license.

immunoglobulin for treating sepsis, severe sepsis and septic shock. *Cochrane Database Syst. Rev.* CD001090 (2013). doi:10.1002/14651858.CD001090.pub2

54. Kaul, R. *et al.* Intravenous immunoglobulin therapy for streptococcal toxic shock syndrome--a comparative observational study. The Canadian Streptococcal Study Group. *Clin. Infect. Dis.* **28,** 800–807 (1999).
55. Darenberg, J. *et al.* Intravenous immunoglobulin G therapy in streptococcal toxic shock syndrome: a European randomized, double-blind, placebo-controlled trial. *Clin. Infect. Dis.* **37,** 333–340 (2003).
56. Kaul, R., McGeer, A., Low, D. E., Green, K. & Schwartz, B. Population-based surveillance for group A streptococcal necrotizing fasciitis: Clinical features, prognostic indicators, and microbiologic analysis of seventy-seven cases. Ontario Group A Streptococcal Study. *Am. J. Med.* **103,** 18–24 (1997).
57. Norrby-Teglund, A. *et al.* Plasma from patients with severe invasive group A streptococcal infections treated with normal polyspecific IgG inhibits streptococcal superantigen-induced T cell proliferation and cytokine production. *J. Immunol.* **156,** 3057–3064 (1996).
58. Skansén-Saphir, U., Andersson, J., Björk, L. & Andersson, U. Lymphokine production induced by streptococcal pyrogenic exotoxin-A is selectively down-regulated by pooled human IgG. *Eur. J. Immunol.* **24,** 916–922 (1994).
59. Andersson, U., Björk, L., Skansén-Saphir, U. & Andersson, J. Pooled human IgG modulates cytokine production in lymphocytes and monocytes. *Immunol. Rev.* **139,** 21–42 (1994).
60. Collin, M. & Fischetti, V. A. A novel secreted endoglycosidase from *Enterococcus faecalis* with activity on human immunoglobulin G and ribonuclease B. *J. Biol. Chem.* **279,** 22558–22570 (2004).
61. Muramatsu, H. *et al.* Molecular cloning and expression of endo-beta-N-acetylglucosaminidase D, which acts on the core structure of complex type asparagine-linked oligosaccharides. *J. Biochem.* **129,** 923–928 (2001).
62. Shadnezhad, A. *et al.* EndoSd: an IgG glycan hydrolyzing enzyme in *Streptococcus dysgalactiae* subspecies *dysgalactiae*. *Future Microbiol*. **11,** 721–736 (2016).
63. Flock, M., Frykberg, L., Sköld, M., Guss, B. & Flock, J.-I. Antiphagocytic function of an IgG glycosyl hydrolase from Streptococcus equi subsp. equi and its use as a vaccine component. *Infect. Immun.* **80,** 2914–2919 (2012).
64. Malmström, E. *et al.* Large-scale inference of protein tissue origin in gram-positive sepsis plasma using quantitative targeted proteomics. *Nat. Comms.* **7,** 10261 (2016).
65. Lange, V., Picotti, P., Domon, B. & Aebersold, R. Selected reaction monitoring for quantitative proteomics: a tutorial. *Mol. Syst. Biol.* **4,** 222 (2008).
66. MacLean, B. *et al.* Skyline: an open source document editor for creating and analyzing targeted proteomics experiments. *Bioinformatics* **26,** 966–968 (2010).
67. MacLean, B. *et al.* Effect of collision energy optimization on the measurement of peptides by selected reaction monitoring (SRM) mass spectrometry. *Anal. Chem.* **82,** 10116–10124 (2010).
68. Collin, M. & Olsén, A. Generation of a mature streptococcal cysteine proteinase is dependent on cell wall-anchored M1 protein. *Mol. Microbiol.* **36,** 1306–1318 (2000).
69. Walker, M. J. *et al.* DNase Sda1 provides selection pressure for a switch to invasive group A streptococcal infection. *Nat. Med.* **13,** 981–985 (2007).
70. Fiebig, A. *et al.* Comparative genomics of *Streptococcus pyogenes* M1 isolates differing in virulence and propensity to cause systemic infection in mice. *Int. J. Med. Microbiol.* **305,** 532–543 (2015).
71. Påhlman, L. I. *et al.* Streptococcal M protein: a multipotent and powerful inducer of

bioRxiv preprint doi: https://doi.org/10.1101/544064; this version posted February 13, 2019. The copyright holder for this preprint (which was not certified by peer review) is the author/funder, who has granted bioRxiv a license to display the preprint in perpetuity. It is made available under aCC-BY-NC-ND 4.0 International license.

inflammation. *J. Immunol.* **177,** 1221–1228 (2006).

72. Shannon, O. *et al.* Severe streptococcal infection is associated with M protein-induced platelet activation and thrombus formation. *Mol. Microbiol.* **65,** 1147–1157 (2007).

bioRxiv preprint doi: https://doi.org/10.1101/544064; this version posted February 13, 2019. The copyright holder for this preprint (which was not certified by peer review) is the author/funder, who has granted bioRxiv a license to display the preprint in perpetuity. It is made available under aCC-BY-NC-ND 4.0 International license.

Figures

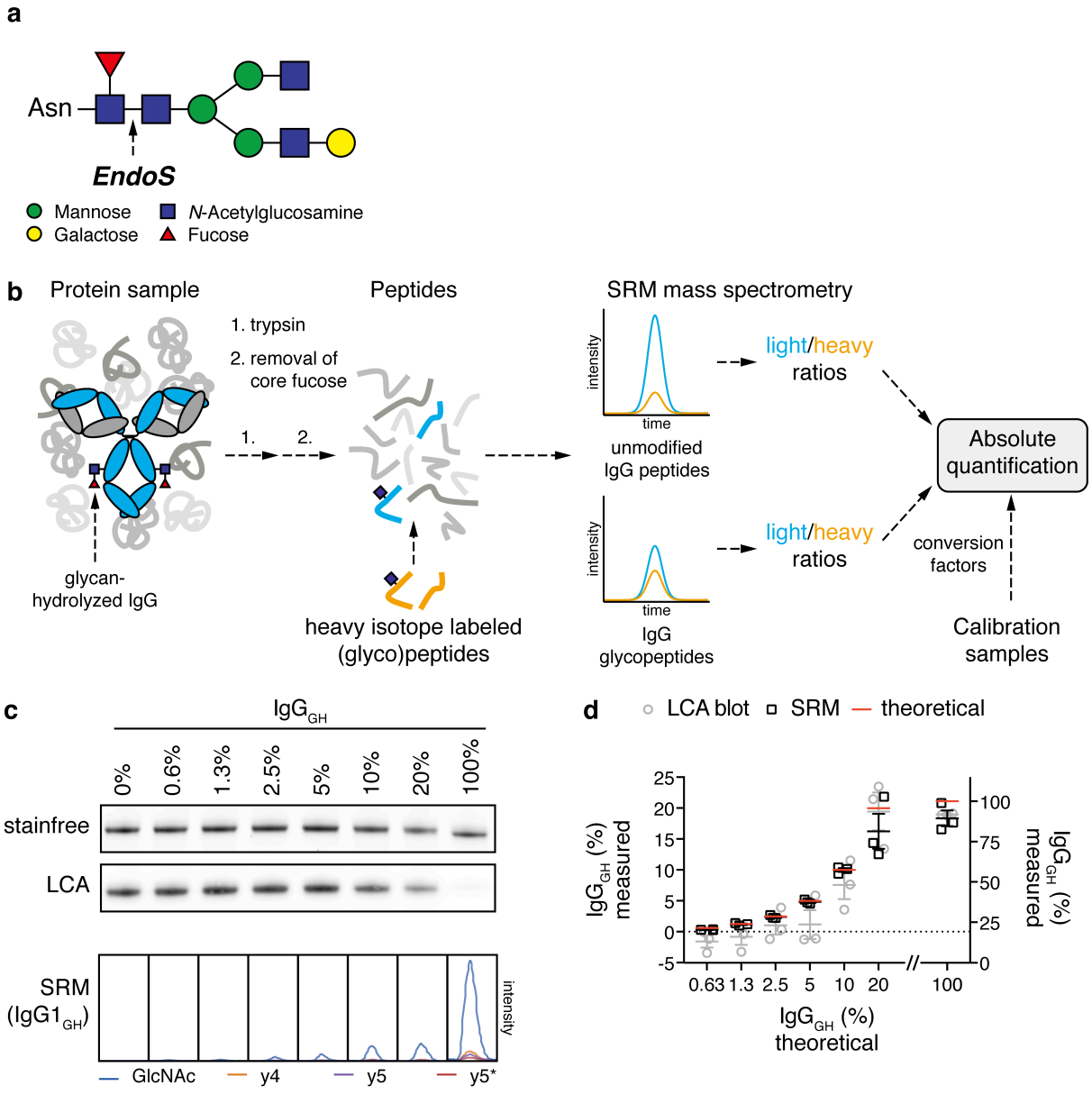

FIGURE 1: TARGETED MASS SPECTROMETRY TO QUANTIFY IGG GLYCAN HYDROLYSIS

a) Typical *N*-glycan structure found on N297 of human IgG antibodies. The arrow marks the EndoS cleavage site in the chitobiose core of the glycan. The EndoS reaction product is an IgG carrying either a single GlcNAc or a GlcNAc-Fucose disaccharide, depending on the core fucosylation status of the antibody.

b) Overview of the SRM-MS method. Complex protein samples are digested to peptides using trypsin and potential core fucosylation is removed using α-fucosidase. The resulting peptide samples are spiked with heavy isotope labeled (glyco)peptide standards corresponding to both subclass specific IgG glycopeptides modified with a single GlcNAc

bioRxiv preprint doi: https://doi.org/10.1101/544064; this version posted February 13, 2019. The copyright holder for this preprint (which was not certified by peer review) is the author/funder, who has granted bioRxiv a license to display the preprint in perpetuity. It is made available under aCC-BY-NC-ND 4.0 International license.

residue as well as subclass specific unmodified peptides. This peptide mixture is analyzed by SRM mass spectrometry resulting in light/heavy ratios for each of the peptides of interest. The absolute amount (concentration) of each IgG subclass as well as the amount of IgG_{GH} is derived from the obtained ratios, using conversion factors determined from a defined set of standard samples

c&d) Validation of SRM-MS quantitative accuracy. A set of plasma samples with defined percentages of IgG_{GH} was prepared by dilution of EndoS-treated plasma with untreated control plasma. The samples were analyzed separately in triplicate by SDS-PAGE/LCA blotting and SRM mass spectrometry. Raw data from both methods is shown in panel c. For the SRM method the chromatograms originating from the glycan-hydrolyzed IgG1 glycopeptide are shown, each transition in a different color. The asterisk denotes a fragment ion that has undergone a neutral loss of the GlcNAc modification. The degree of IgG glycan hydrolysis in the standard sample set was quantified using both methods (panel d). The red line marks the theoretical value and the measured values are depicted in grey circles (LCA blot) and black boxes (SRM) respectively. The means and standard errors are plotted and each individual data point is marked with a circle or box. The first 6 values are plotted on the left z-axis, the final 100% IgG_{GH} sample on the right y-axis.

bioRxiv preprint doi: https://doi.org/10.1101/544064; this version posted February 13, 2019. The copyright holder for this preprint (which was not certified by peer review) is the author/funder, who has granted bioRxiv a license to display the preprint in perpetuity. It is made available under aCC-BY-NC-ND 4.0 International license.

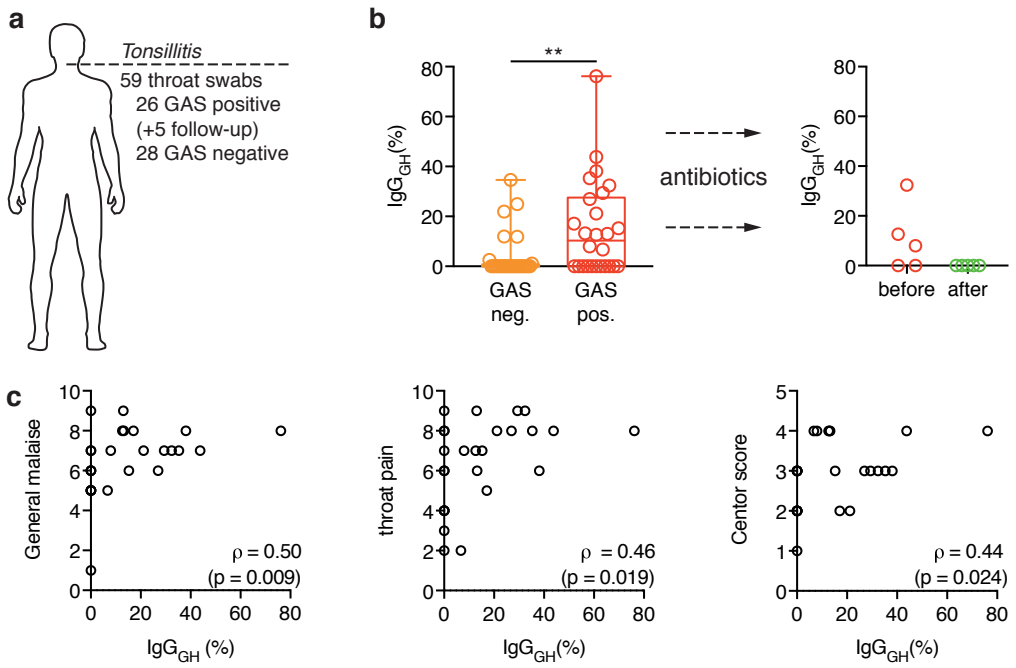

FIGURE 2: IGG GLYCAN HYDROLYSIS DURING GAS TONSILLITITS

a) Overview of the collected throat swab samples from patients seeking medical attention for a sore throat. A total of 59 samples were taken from 54 different patients (26 GAS positive tonsillitis, 28 GAS negative tonsillitis). Follow-up refers to additional samples that were taken from 5 of the GAS tonsillitis patients after antibiotic treatment.

b) Percentage of glycan-hydrolyzed IgG as determined by SRM-MS analysis of tonsillar swabs from patients with, either GAS-negative (orange) or GAS-positive (red) tonsillitis. The boxes represent the 25th to 75th percentile with the median depicted as a line in the middle. The whiskers reach from the smallest to the largest data point, all of which are marked as circles. Glycan hydrolysis of the individual subclasses is shown in table S4. The glycopeptides from IgG3 and IgG4 could not be measured in these samples due to interfering background and were omitted from this analysis. Data was analyzed using a Mann-Whitney test (Table S6) (ns: $p>0.05$, **: $p<0.01$).

c) The tonsillitis patients were asked to grade their a general malaise (left) and throat pain (middle) on a scale from 0-10 and the centor score[38] (right) was determined. These parameters were correlated to the IgG glycan hydrolysis measured in tonsillar swabs using SRM-MS. Correlation was analyzed according to Spearman (Table S7).

bioRxiv preprint doi: https://doi.org/10.1101/544064; this version posted February 13, 2019. The copyright holder for this preprint (which was not certified by peer review) is the author/funder, who has granted bioRxiv a license to display the preprint in perpetuity. It is made available under aCC-BY-NC-ND 4.0 International license.

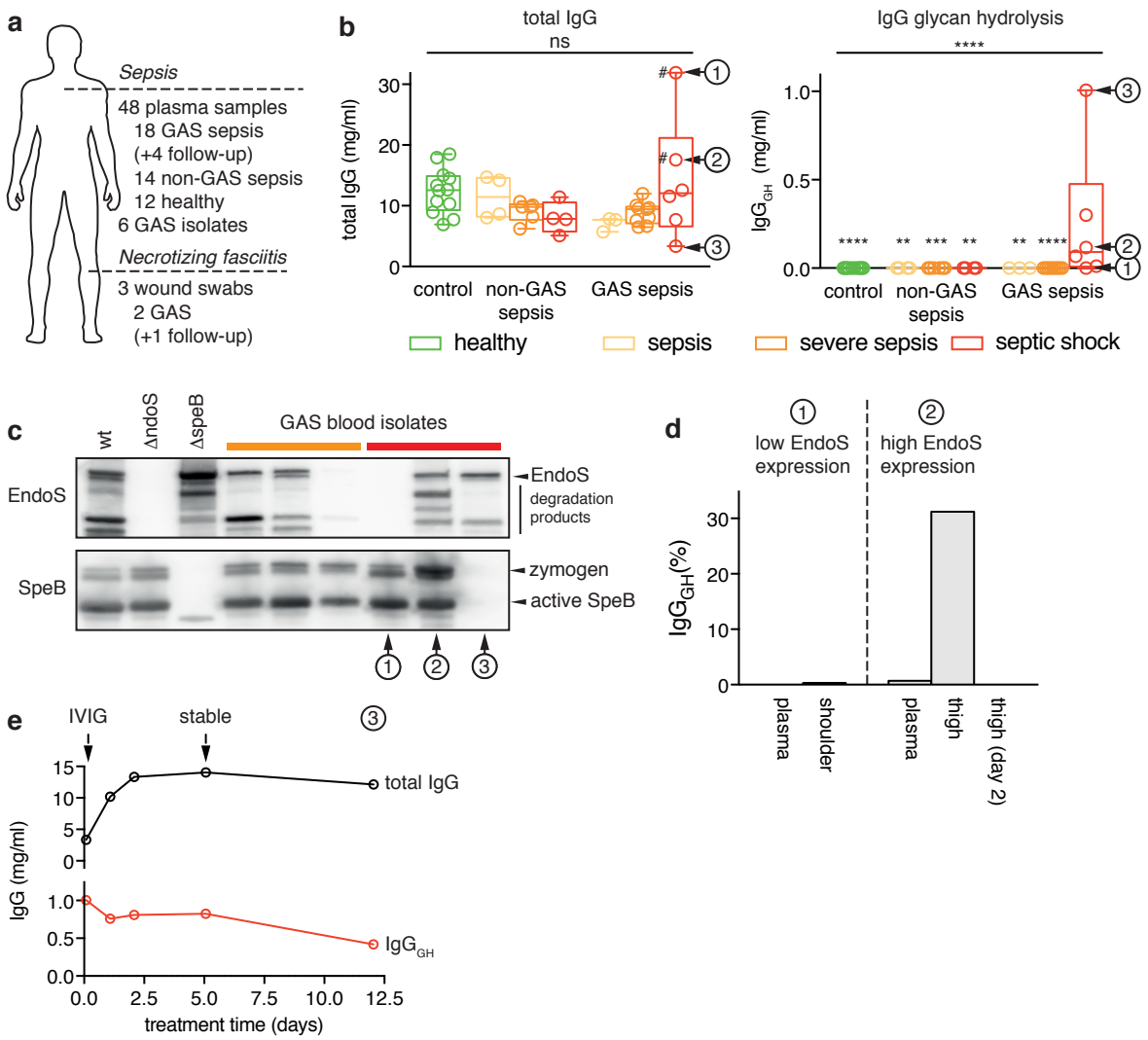

848

849 FIGURE 3: IGG GLYCAN HYDROLYSIS DURING INVASIVE GAS INFECTION

850 a) Overview of the collected samples from sepsis patients. A total of 48 plasma samples, 3
851 wound swabs and 6 GAS isolates was collected from 32 patients (18 GAS sepsis, 14 non-
852 GAS sepsis) and 12 healthy control individuals. Follow-up refers to 4 additional plasma
853 samples that were taken from the same patient during the course of treatment and recovery.

854 b) Plasma concentration of total IgG (left panel) as well as the glycan-hydrolyzed IgG (right
855 panel) as determined by SRM-MS. The patients are grouped according to infection state
856 (healthy, non-GAS sepsis, GAS sepsis), as well as sub-grouped according to severity of
857 disease (sepsis, severe sepsis, septic shock). The boxes represent the 25th to 75th percentile
858 with the median depicted as a center line. The whiskers reach from the smallest to the largest
859 data point, all of which are marked as circles. Glycan hydrolysis of the individual subclasses
860 is shown in table S5. The p-value of the overall comparison of all the groups (by Kruskal-
861 Wallis test) as well as adjusted p-values for the individual comparisons of the GAS septic

bioRxiv preprint doi: https://doi.org/10.1101/544064; this version posted February 13, 2019. The copyright holder for this preprint (which was not certified by peer review) is the author/funder, who has granted bioRxiv a license to display the preprint in perpetuity. It is made available under aCC-BY-NC-ND 4.0 International license.

shock group with each of the other groups are depicted (ns: $p>0.05$, *: $p<0.05$, **: $p<0.01$, ***: $p<0.001$, ****: $p<0.0001$). For a more detailed description of the statistical analysis see tables S8&S9). Two patients (marked by the hashtag #) had received IVIG treatment before the sample was drawn, affecting their total IgG concentrations. From three patients (marked 1-3) additional samples could be obtained and their analysis is shown in the other panels of this figure.

c) Expression of EndoS and SpeB by clinical GAS isolates *in vitro*. Blood culture isolates from patients 1-3 as well as three patients from the GAS severe sepsis group were analyzed with respect to their ability of secrete EndoS (top panel) and SpeB (bottom panel) into the culture supernatant *in vitro*. The culture supernatants were analyzed by SDS-PAGE followed by immunoblotting using rabbit antisera specific to EndoS and SpeB respectively. AP1 (wt) and isogenic *ndoS* and *speB* mutants were used as positive and negative controls respectively.

d) Local vs. systemic glycan hydrolysis. From patients 1 & 2, wound swab samples from the site of infection (patient 1: shoulder and patient 2: thigh) could be obtained and were analyzed by SRM-MS. The percentage of IgG_{GH} in the tissue as well as in plasma is shown.

e) IgG glycan hydrolysis over the course of infection. A series of plasma samples from patient 3 (starting at 2h after admission until 12 days later) was analyzed using SRM-MS. Both the concentration of total IgG (black) as well as IgG_{GH}(red) is shown. The arrows mark onset of IVIG treatment (4h) and the time point when the patient was stable (5 days).

bioRxiv preprint doi: https://doi.org/10.1101/544064; this version posted February 13, 2019. The copyright holder for this preprint (which was not certified by peer review) is the author/funder, who has granted bioRxiv a license to display the preprint in perpetuity. It is made available under aCC-BY-NC-ND 4.0 International license.

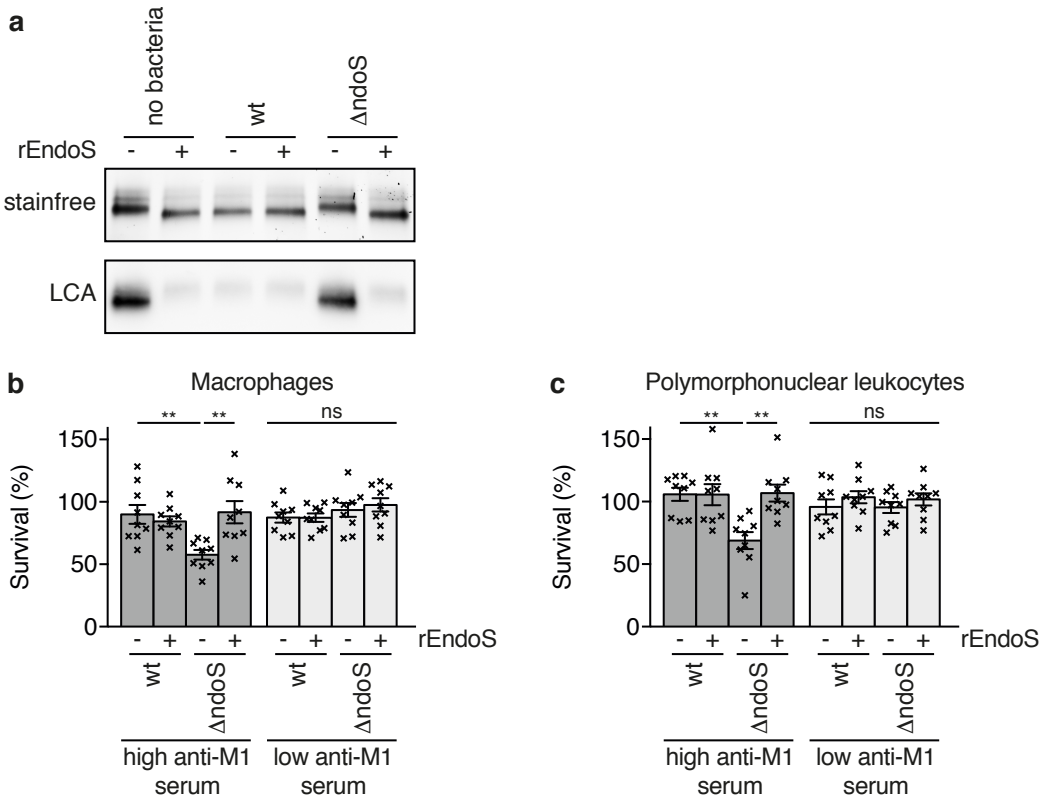

FIGURE 4: ENDOS CONFERS RESISTANCE TO PHAGOCYTIC KILLING

a) GAS 5448 and an isogenic *ndoS* mutant were grown in human saliva supplemented with 5% human serum. IgGs were purified by Protein G and analyzed by SDS-PAGE (top) and LCA blot (bottom). Addition of recombinant EndoS (rEndoS) was used to complement the mutation.

b) Saliva-grown GAS 5448 and an isogenic *ndoS* mutant were challenged with human monocyte-derived macrophages (left) and human polymorphonuclear leukocytes (right) in the presence of serum with a high (dark grey) or low (light grey) anti-M1 IgG response. Survival rates were determined by numerating bacteria both in the initial inoculum as well as after incubation with the phagocytic cells. Data from 3 independent experiments with different cell donors (each preformed in triplicate, total n=9) was combined and analyzed using a Kruskal-Wallis test followed by Dunn´s multiple comparison test (Tables S10-13) (ns: $p>0.05$, **: $p<0.01$). The bar represents the mean, with the standard error depicted as error bars. Each individual data point is represented with a cross, showing the variability between the individual experiments and the replicates within the same experiment.

bioRxiv preprint doi: https://doi.org/10.1101/544064; this version posted February 13, 2019. The copyright holder for this preprint (which was not certified by peer review) is the author/funder, who has granted bioRxiv a license to display the preprint in perpetuity. It is made available under aCC-BY-NC-ND 4.0 International license.

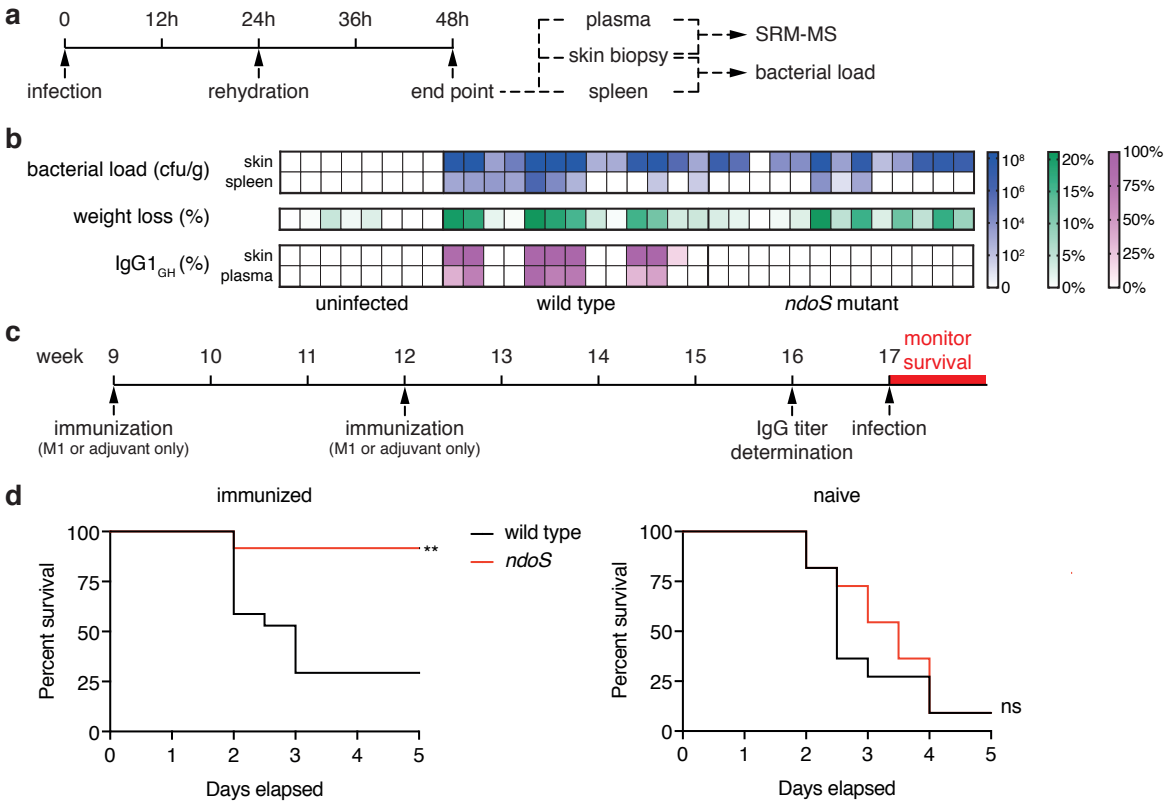

FIGURE 5: ENDOS LEADS TO IGG GLCYANS HYDROLYSIS AND CONFERS A SELECTIVE ADVANTAGE IN A MOUSE MODEL OF GAS INFECTION

a) Experimental setup for the infections of immunologically naïve mice. 9 week old, female C57BL/6 mice were infected subcutaneously in the flank with GAS AP1, an *ndoS* mutant or PBS. The animals were rehydrated by injection of 0.5 ml saline at 24 h and sacrificed at 48 h post infection. The spleen and a skin biopsy from the site of injection were taken to assess bacterial loads and the skin sample, as well as a plasma sample were used for analysis by SRM-MS.

b) Bacterial load (blue), weight loss (green) and percentage of IgG1 glycan hydrolysis as determined by SRM-MS (purple) at 48h post infection. Each column corresponds to an individual animal.

c) Experimental setup for the immunization with M1 and subsequent infection of mice. 9 week old, female C57BL/6 mice were injected with purified M1 protein or adjuvant only and received a second dose at 12 weeks of age. After 4 weeks, the anti-M1 IgG response was assessed by ELISA and the animals were infected subcutaneously one week later.

d) Survival of M1-immunized (right) and mock-immunized (left) animals after infection with either GAS AP1 wild-type (black) or *ndoS* mutant (red). Mice were monitored twice

bioRxiv preprint doi: https://doi.org/10.1101/544064; this version posted February 13, 2019. The copyright holder for this preprint (which was not certified by peer review) is the author/funder, who has granted bioRxiv a license to display the preprint in perpetuity. It is made available under aCC-BY-NC-ND 4.0 International license.

daily for survival for a period of 5 days. Curves were compared using a Mantel-Cox test (ns: $p>0.05$, **: $p<0.01$).